

Andreas H. Mahnken
Philipp Bruners
Marcus Katoh
Joachim E. Wildberger
Rolf W. Günther
Arno Buecker

Dynamic multi-section CT imaging in acute myocardial infarction: preliminary animal experience

Received: 16 June 2005

Revised: 24 September 2005

Accepted: 7 October 2005

Published online: 9 November 2005

© Springer-Verlag 2005

A. H. Mahnken (✉) · P. Bruners ·
M. Katoh · J. E. Wildberger ·
R. W. Günther · A. Buecker
Department of Diagnostic Radiology,
RWTH Aachen University,
Pauwelsstrasse 30,
D-52074 Aachen, Germany
e-mail: mahnen@rad.rwth-aachen.de
Tel.: +49-241-8088332
Fax: +49-241-8082499

Abstract To evaluate the feasibility of myocardial first-pass perfusion imaging with multidetector CT (MDCT). In five pigs, myocardial infarction was induced by permanent balloon occlusion of the left anterior descending coronary artery. Dynamic contrast-enhanced MDCT (12×1.5 mm, 120 kV, 30 mAs, 64 acquisitions, 40 ml iopromide 370@4ml/s) and contrast-enhanced first-pass perfusion magnetic resonance (MR) imaging (TR 7.7 ms/TE 2.6 ms, 64 acquisitions, 0.05 mmol/kg Gd-DTPA) were performed. Finally, the animals were sacrificed, and the heart was excised and stained with triphenyltetrazoliumchloride (TTC). Maximum signal intensity (SI_{max}), contrast material arrival time (CAT), wash-in time (T_{max}) and slope were calculated from time-density/signal-intensity curves. The area of myocardial hypoperfusion was measured as the percentage of the left-ventricular area (%LV).

Parameters were compared using Bland-Altman plots and Student's *t*-tests. The hypoperfused area on MDCT was $19.3 \pm 4.5\%$ LV (MR imaging $17.2 \pm 4.0\%$ LV). The mean size of infarction was $18.7 \pm 5.7\%$ LV with TTC. Semiquantitative analysis of MR imaging and MDCT for SI_{max} , T_{max} and slope showed significant differences between normal and infarcted myocardium ($P < 0.05$). No significant differences were found for CAT. MDCT and MR imaging both allowed for the differentiation of hypoperfused and normal myocardium. Results given in absolute values differed significantly between both imaging modalities ($P < 0.05$). MDCT has the potential for visual and semiquantitative assessment of first-pass myocardial perfusion.

Keywords Computed tomography · Heart perfusion · Myocardial infarction

Introduction

Despite the widespread use of coronary angiography for the diagnosis of coronary artery disease (CAD), the significance of a coronary artery lesion may vary, resulting in the need for other techniques to assess the physiological relevance. Decreased myocardial perfusion represents the first effect of obstructive CAD [1]. Consequently, imaging modalities depicting myocardial perfusion are clinically useful diagnostic tools. Searching for myocardial ischemia, first-pass myocardial perfusion imaging is suited to assess

the functional impact of coronary artery stenosis. First-pass perfusion imaging allows the detection of impaired microvascular function. With magnetic resonance (MR) imaging, it can be detected non-invasively even in patients with normal findings on coronary angiography [2].

With the introduction of electrocardiogram (ECG)-gated multidetector row computed tomography (MDCT) into the clinical routine, non-invasive assessment of the coronary arteries became feasible [3]. Moreover, this technique allows the assessment of cardiac function at rest [4]. Only recently, several studies showed the potential of MDCT to

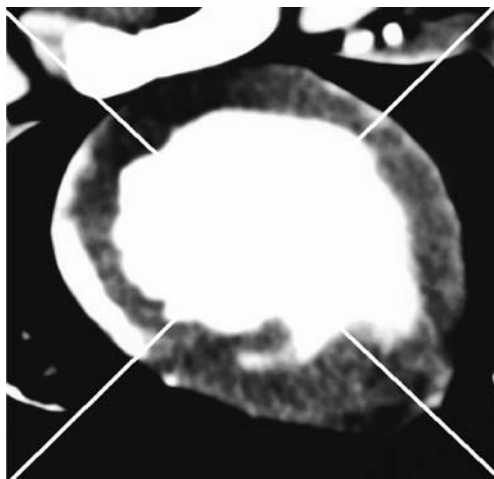


Fig. 1 Axial MDCT image of a pig heart. For data analysis, myocardium of each slice was divided into four equally sized segments. Straight lines perpendicular to the attachment of the right ventricular wall to the left ventricle were used to separate the segments

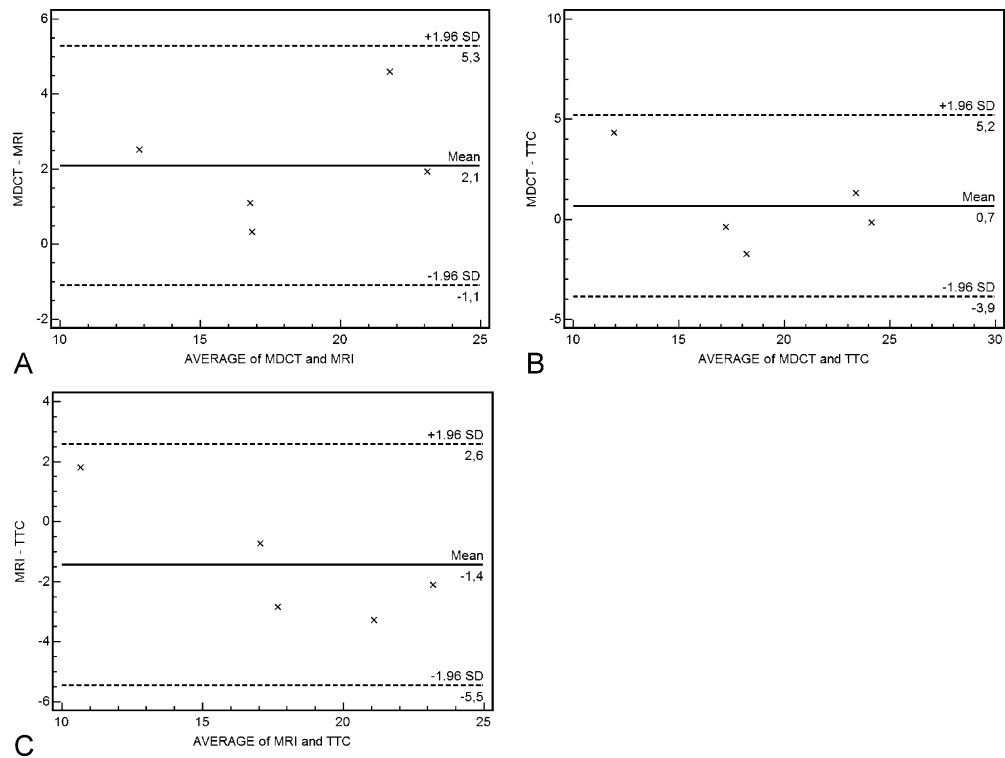
assess myocardial infarction from decreased myocardial contrast enhancement during the arterial phase as well as from delayed myocardial contrast enhancement [5–11]. However, dynamic first-pass MDCT imaging has not been evaluated yet. Therefore, the aim of this study was to assess the feasibility of dynamic myocardial first-pass perfusion imaging with cardiac MDCT in an animal model.

Material and methods

Animal preparation

Five domestic pigs weighting 56 to 61 kg (mean: 57.3 ± 4.3 kg) were included in this study after approval from the official committee on animal affairs. Following intramuscular pre-medication with 0.5 mg atropine (atropinum sulfuricum solutum 1%, WDT, Garbsen, Germany), 0.2 mg azaperone (Stresnil, Janssen-Cilag, Neuss, Germany) and 0.1 mg ketamine/kg bodyweight (Ketamin 10%, Ceva Tiergesundheit, Düsseldorf, Germany), pentobarbital solution (Narcoren, Merial, Hallbergmoos, Germany) diluted with saline (1:3) was administered as needed via an 18-G venous access line placed in an ear vein. No additional medication was applied, especially no drugs to reduce the heart rate. The animals were intubated and mechanically ventilated. Under fluoroscopy guidance, a 7-F guiding catheter (Vista Brite Tip, Cordis, Miami Lakes, FL, USA) was placed at the origin of the left coronary artery, and a coronary angiogram was obtained. Afterwards permanent balloon occlusion of the left anterior descending (LAD) coronary artery was performed at mid-section. The balloon catheter size (Hayate, Terumo, Tokyo, Japan) was individually adapted to the vessel size, ranging from 2.5 to 3.0 mm. Coronary artery occlusion was controlled with coronary angiograms before and after the imaging procedures.

Fig. 2 Bland-Altman plots show the agreement of the infarct size between MDCT and MR imaging (a), MDCT and TTC staining (b) as well as MR imaging and TTC staining (c)

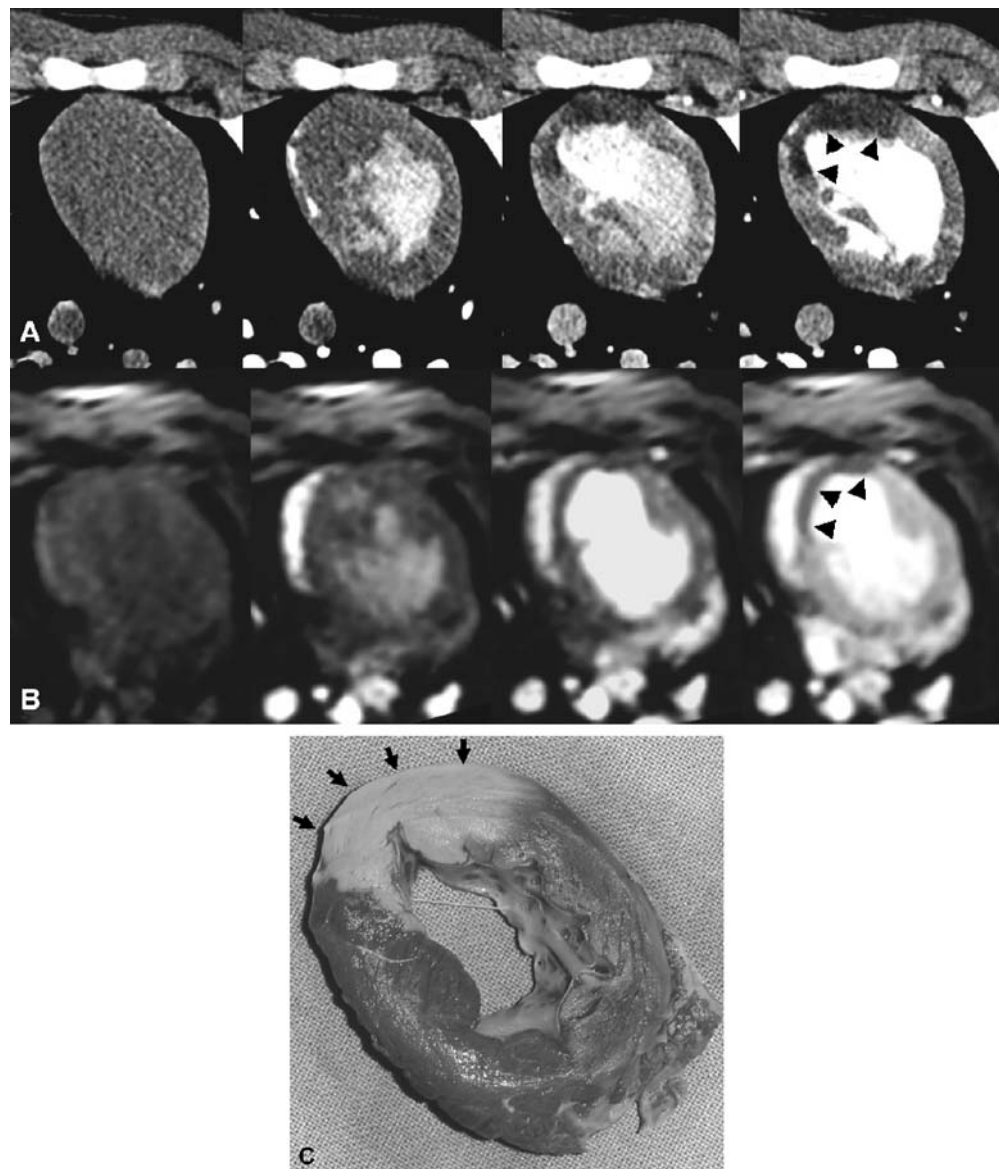


MR imaging

MR imaging was performed 45 min after LAD occlusion. MR studies were performed on a 1.5-T whole body MR scanner (Gyroscan Intera, Philips Medical Systems, Best, The Netherlands) using a five-element cardiac synergy coil. All animals were examined in the supine position, assessing the same myocardial region as with MDCT. For first-pass imaging, 0.05 mmol/kg bodyweight gadopentate dimeglumine (Magnevist, Schering, Berlin, Germany) was injected via an ear vein at a flow rate of 4 ml/s and a T1-weighted multislice gradient echo echoplanar imaging (EPI) sequence was used. Imaging parameters were chosen as follows: TR (repetition time)=7.7 ms, TE (echo time)= 2.6 ms,

flip-angle=20°, FOV=350×350 mm², 128×128 matrix and 64 acquisitions. The acquisition time for the EPI readout was 69 ms with a temporal resolution of one RR interval, resulting in a total acquisition time of 45 s at a heart rate of 87 beats per minute (bpm). Three images with a slice thickness of 8 mm without an interslice gap were acquired with an orientation corresponding to the MDCT images. To assess the steady state of the magnetization, at least five images were acquired before the contrast material reached the heart. Window settings were visually adapted depending on the individual image contrast.

Fig. 3 MDCT (a) and MR (b) images present with a hypoenhancement (arrowheads) of the infarcted left ventricular myocardium, while non-infarcted myocardium presents with regular contrast enhancement. TTC staining (c) confirms extents and location of MI (arrows)



MDCT examination

On average, MDCT scans started 15 min (range: 13–18 min) after the MR examination. All CT examinations were performed with a 16-MDCT scanner (SOMATOM Sensation 16, release VA 50, Siemens, Forchheim, Germany) in the supine position during end-expiratory breath-hold. Serial CT scanning in the axial plane was performed at the level of the left ventricular apex after bolus injection of 40 ml of non-ionic contrast material (Ultravist 370, Schering) followed by a 30-ml saline chaser bolus, both injected at a flow rate of 4 ml/s. Sixty-four scans were acquired applying a prospectively ECG-triggered examination protocol with 12×1.5 -mm collimation, 0-mm table feed per rotation and a tube rotation time of 420 ms. Tube voltage was 120 kV with 30 mAs. The trigger point was set to 60% of the RR interval. Ventilation was suspended for a total of 38 s.

From each acquisition, three images were reconstructed with an effective slice thickness of 6.0 mm. A field-of-view (FOV) of 150×150 mm², a 512×512 reconstruction matrix and a medium-smooth convolution kernel (B30f) were chosen. A window width of 400 Hounsfield units (HU) with a window center of 80 HU was applied. The CTDI_{Vol} was 139.35 mGy. The effective radiation dose was not determined as this was an animal study.

Immediately after the MDCT examination, the animals were sacrificed, and the heart was excised and instantly sectioned into 8-mm-thick axial slices. The slices were stained with 2% 2,3,5-triphenyltetrazolin-chloride (TTC) and photographed at 600 dpi with a commercially available digital camera.

Data analysis

From MR imaging and MDCT, two sections were selected for data analysis. Each of these slices was divided into four segments. Straight lines perpendicular to the attachment of the right ventricular wall to the left ventricle were used to separate the four segments (Fig. 1). Two sections with 4 segments each in five animals resulted in a total of 40 segments. From MDCT and MR imaging, time-density/signal-intensity (SI) curves were calculated for each of these segments as well as for the left ventricular cavum, applying manually drawn regions-of-interest that were individually adapted to the shape of the myocardium. After baseline correction, signal intensity/attenuation was expressed as the percentage of increase over baseline SI/attenuation. From this data, the following parameters were calculated for both imaging modalities [12]:

- maximum signal intensity (SI_{max})=the maximum signal intensity/attenuation during the first pass of the contrast material;

- contrast material arrival time (CAT)=the difference between the contrast enhancement of the left ventricular cavum and the myocardium;
- wash-in time (T_{max})=the difference between the beginning of the myocardial contrast enhancement and the point of maximum contrast enhancement;
- slope = the maximum slope of five consecutive measurements during the wash-in period of the contrast material calculated from a linear fit.

To correct the data for variations in the hemodynamic state, all values were divided by the values calculated for the left ventricular cavum.

The size of the hypoperfusion was calculated as the percentage of left ventricular area per slice (%LV) for MR imaging and MDCT from the manually drawn regions-of-interest. The infarct size was measured from TTC staining.

All values are given as the mean±standard deviation. The size of MI was compared with Bland-Altman plots. First-pass perfusion results were evaluated using a paired Student's *t*-test. A *P*-value<0.05 was considered statistically significant.

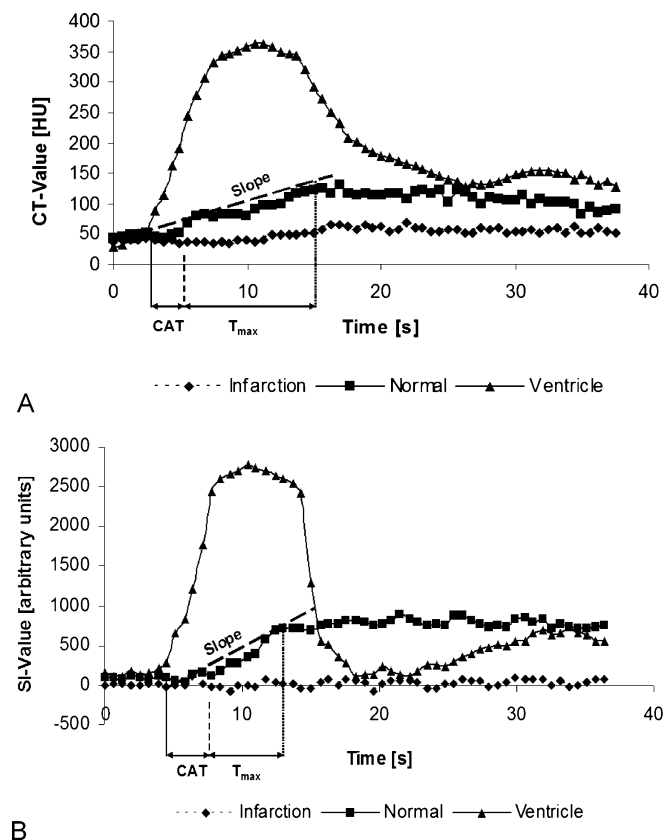


Fig. 4 Time-density curves for MDCT (a) and time-SI curves for MRI (b) demonstrate missing contrast enhancement in the area of myocardial infarction. Although the curves reflect differences between both imaging modalities, both techniques show an identical contrast enhancement pattern, differentiating normal from infarcted myocardium

Table 1 Results of the semiquantitative analysis of the time-density/signal-intensity curves show significant differences between infarcted and healthy myocardium for SI_{max} , T_{max} and slope

		Infarction	Normal	P-value
SI _{max}	MDCT	0.07±0.02	0.17±0.05	>0.001
	MRI	0.04±0.01	0.30±0.04	>0.001
CAT	MDCT	1.94±0.73	0.69±0.12	0.021
	MRI	1.07±0.43	0.62±0.18	0.056
T _{max}	MDCT	3.08±0.57	1.33±0.18	0.005
	MRI	2.33±0.42	1.54±0.37	>0.001
Slope	MDCT	0.003±0.001	0.18±0.03	>0.001
	MRI	0.001±0.001	0.13±0.04	0.001

Results

In one animal, left ventricular fibrillation occurred 17 min after coronary balloon occlusion that was successfully treated with direct current defibrillation. All animals underwent complete MDCT and MR examinations. The mean heart rate during MDCT was 87.0±11.2 bpm.

The hypoperfused area was 19.3±4.5%LV calculated from MDCT and 17.2±4.0%LV on MR. Mean infarct size was 18.7±5.7%LV on TTC staining. Bland-Altman plots showed no systematic error, with a mean difference ranging from -1.4 to 2.1 %LV (Fig. 2).

In two animals (=four sections), the septal segment of the left ventricular myocardium had to be excluded from the analysis because of beam-hardening artifacts caused by contrast material passage through the right ventricle. These artifacts resulted in hypo- and hyperdense streak artifacts averting any assessment of the affected myocardium. Thus, 36/40 myocardial segments (90%) were assessable. Visual assessment of MR imaging and MDCT revealed hypoenhancement defined as myocardial ischemia in the identical 10/36 assessable segments. TTC staining proved the presence of myocardial infarction in these segments (Fig. 3). For MR imaging as well as for MDCT analysis of SI_{max} , the T_{max} and slope showed significant differences between normal and infarcted myocardium. For CAT, no significant differences were found. Furthermore, absolute values showed significant differences between MR imaging and MDCT results ($P<0.001$). Fig. 4 shows time-density/SI curves for MDCT and MR imaging. In detail, results for the semiquantitative analysis of the contrast enhancement are given in Table 1.

Discussion

First-pass myocardial perfusion imaging has the potential to detect impaired microvascular function prior to the occurrence of clinical symptoms like ECG changes or wall motion abnormalities [1]. Currently, imaging of myocardial perfusion is dominated by single photon emission tomog-

raphy (SPECT), while positron emission tomography has to be considered as the gold standard for perfusion imaging. MR imaging is becoming an accepted alternative to nuclear medicine techniques [10]. While the use of electron beam computed tomography for the assessment of myocardial perfusion was shown about 20 years ago [13], cardiac MDCT only recently has proved its potential to depict myocardial infarction from hypo-enhanced myocardium [5, 14, 15]. So far, there are no data available on the use of cardiac MDCT for the dynamic assessment of first-pass myocardial perfusion. Therefore, the particular innovation of the presented study is the introduction of dynamical multi-phase imaging in cardiac MDCT with myocardial contrast enhancement over time interpreted as myocardial perfusion. This approach adds valuable information on myocardial perfusion imaging when compared to the assessment of myocardial perfusion from single arterial phase imaging [14, 15].

When compared to MR imaging, MDCT perfusion imaging offers several theoretical advantages, like the linear relation between contrast enhancement and iodine concentration, which potentially allows for the direct quantification of myocardial blood flow, avoiding the need for potentially error-bearing correction methods. In combination with MDCT coronary angiography and functional analysis, MDCT holds the potential of a single comprehensive examination of the heart. Further advantages of MDCT include its widespread availability and its ease of use. The main limitation of MDCT is its limited temporal resolution, which hampers the application of MDCT in stress examinations at increased heart rates. This is important as a temporal resolution of one image per RR interval is needed for the generation and quantification of a sufficient arterial input function [16]. So far, MR imaging with the EPI technique offers a relevant advantage for MDCT with respect to the temporal resolution. Moreover, dynamic MDCT data acquisition results in an increased radiation exposure when compared to single phase MDCT that is routinely performed for coronary MDCT angiography. An additional exposure to contrast material is also needed. The combination of rest and stress MDCT perfusion imaging will further increase the radiation and contrast material load to the patient. In contrast, MR imaging is well established for the assessment of myocardial perfusion, allowing for stress testing at higher heart rates. In addition, the latter avoids repeated patient exposure to radiation and potentially nephrotoxic contrast material. So far, however, MR perfusion imaging is no clinical standard, although the benefits of this technique have long been known. In contrast, the feasibility of dynamic first-pass MDCT imaging has only been shown in an experimental setting. Considering its specific limitations, it is only suited for patients with contraindications for MR imaging like pacemakers or cardiac metal. Nevertheless, in combination with coronary MDCT angiography, this technique may hold the potential to detect myocardium

at risk, providing a powerful tool to examine the heart in a single comprehensive examination.

These results indicate that MDCT, despite its limitations, is promising for myocardial perfusion imaging. Moreover, hypo-enhancement was shown to be related directly to myocardial infarction when compared to TTC staining. On MDCT, however, hypo-enhanced regions were slightly larger than the areas of acute myocardial infarction detected by MR imaging or TTC staining. This finding is in agreement with the results reported from other study groups [5, 15] and might be explained by a reduced perfusion in combination with an edema in the peri-infarction zone [17]. As both mechanisms result in lower attenuation values when compared with healthy myocardium [18], these mechanisms are likely to contribute to the overestimation of the hypoperfused areas on MDCT. In our study the difference of the infarct size was less between MDCT and MR imaging when compared to the results reported by Nikolaou et al. [15]. This might be due to the different methods of data acquisition. Dynamic MDCT imaging may provide information that is more similar to MR perfusion imaging than arterial phase MDCT. Moreover, the difference between hypoperfused areas on MDCT and infarct size as determined from TTC staining was expected to be larger than actually was found. This finding

might be due to the point of MDCT image reconstruction. According to our experience, the measured infarct size is considerably influenced by the point of image reconstruction.

There are several important limitations of this study. First, only occlusive infarctions with complete vessel occlusion were examined. Thus, SI_{max} , CAT, T_{max} and slope were used as parameters of perfusion in infarcted myocardium instead of myocardium at risk. Second, all examinations were performed at rest only, while stress perfusion imaging has long been known to be more precise for the detection of myocardial perfusion deficits [19]. Third, because of technical limitations, the slice thickness of MDCT and MR images differed. This limitation, however, was overcome by the selection of two identical sections in each animal. Finally, the perfusion deficit was measured using TTC staining alone instead of an additional blue dye injection *in vivo*. However, no difference was to be expected between both techniques as an animal model with total LAD occlusion was used in this study.

In conclusion, aside from several limitations, our preliminary results demonstrate the potential for semi-quantitative evaluation of myocardial first-pass perfusion from dynamic contrast-enhanced cardiac MDCT. These encouraging results warrant further research on cardiac CT perfusion imaging.

References

- Nesto RW, Kowalchuk GJ (1987) The ischemic cascade: temporal sequence of hemodynamic, electrocardiographic and symptomatic expressions of ischemia. *Am J Cardiol* 59:23C–30C
- Panting JR, Gatehouse PD, Yang GZ, Grothues F, Firmin DN, Collins P, Pennell DJ (2002) Abnormal subendocardial perfusion in cardiac syndrome X detected by cardiovascular magnetic resonance imaging. *N Engl J Med* 346:1948–1953
- Ropers D, Baum U, Pohle K, Anders K, Ulzheimer S, Ohnesorge B, Schlundt C, Bautz W, Daniel WG, Achenbach S (2003) Detection of coronary artery stenoses with thin-slice multi-detector row spiral computed tomography and multiplanar reconstruction. *Circulation* 107:664–666
- Mahnken AH, Koos R, Katoh M, Spuentrup E, Busch P, Wildberger JE, Kühl HP, Günther RW (2005) Sixteen-slice spiral CT versus MR imaging for the assessment of left ventricular function in acute myocardial infarction. *Eur Radiol* 15:714–720
- Hoffmann U, Millea R, Enzweiler C, Ferencik M, Gulick S, Titus J, Achenbach S, Kwiat D, Sosnovik D, Brady TJ (2004) Acute myocardial infarction: contrast-enhanced multi-detector row CT in a porcine model. *Radiology* 231:697–701
- Mochizuki T, Murase K, Higashino H, Koyama Y, Azemoto S, Ikezoe J (1999) Images in cardiovascular medicine. Demonstration of acute myocardial infarction by subsecond spiral computed tomography: early defect and delayed enhancement. *Circulation* 99:2058–2059
- Gosalia A, Haramati LB, Sheth MP, Spindola-Franco H (2004) CT detection of acute myocardial infarction. *AJR Am J Roentgenol* 182:1563–1566
- Paul JF, Wartski M, Caussin C, Sigal-Cinqualbre A, Lancelin B, Angel C, Dambrin G (2005) Late defect on delayed contrast-enhanced multi-detector row CT scans in the prediction of SPECT infarct size after reperfused acute myocardial infarction: initial experience. *Radiology* 236:485–489
- Mahnken AH, Koos R, Katoh M, Wildberger JE, Spuentrup E, Buecker A, Gunther RW, Kuhl HP (2005) Assessment of myocardial viability in reperfused acute myocardial infarction using 16-slice computed tomography in comparison to magnetic resonance imaging. *J Am Coll Cardiol* 45:2042–2047
- Barkhausen J, Hunold P, Jochims M, Debatin JF (2004) Imaging of myocardial perfusion with magnetic resonance. *J Magn Reson Imaging* 19:750–757

11. Koyama Y, Matsuoka H, Mochizuki T, Higashino H, Kawakami H, Nakata S, Aono J, Ito T, Naka M, Ohashi Y, Higaki J (2005) Assessment of reperfused acute myocardial infarction with two-phase contrast-enhanced helical CT: prediction of left ventricular function and wall thickness. *Radiology* 235:804–811
12. Al-Saadi N, Gross M, Bornstedt A, Schnackenburg B, Klein C, Fleck E, Nagel E (2001) Comparison of different semiquantitative parameters for the assessment of a myocardial perfusion reserve index by magnetic resonance imaging. *Z Kardiol* 90:824–834
13. Rumberger JA, Feiring AJ, Lipton MJ, Higgins CB, Ell SR, Marcus ML (1987) Use of ultrafast computed tomography to quantitate regional myocardial perfusion: a preliminary report. *J Am Coll Cardiol* 9:59–69
14. Francone M, Carbone I, Danti M, Lanciotti K, Cavacece M, Mirabelli F, Gaudio C, Catalano C, Passariello R (2005) ECG-gated multi-detector row spiral CT in the assessment of myocardial infarction: correlation with non-invasive angiographic findings. *Eur Radiol* Jun 14; [Epub ahead of print]. DOI 10.1007/s00330-005-2800-3
15. Nikolaou K, Sanz J, Poon M, Wintersperger BJ, Ohnesorge B, Rius T, Fayad ZA, Reiser MF, Becker CR (2005) Assessment of myocardial perfusion and viability from routine contrast-enhanced 16-detector-row computed tomography of the heart: preliminary results. *Eur Radiol* 15:864–871
16. Kroll K, Wilke N, Jerosch-Herold M, Wang Y, Zhang Y, Bache RJ, Bassingthwaite JB (1996) Modeling regional myocardial flows from residue functions of an intravascular indicator. *Am J Physiol* 271:H1643–1655
17. Saeed M, Lund G, Wendland MF, Bremerich J, Weinmann HJ, Higgin CB (2001) Magnetic resonance characterization of the peri-infarction zone of reperfused myocardial infarction with necrosis-specific and extracellular non-specific contrast media. *Circulation* 103:871–876
18. Skioldebrand CG, Lipton MJ, Redington RW, Berninger WH Wallace A, Carlsson E (1981) Myocardial infarction in dogs, demonstrated by non-enhanced computed tomography. *Acta Radiol Diagn* (Stockh) 22:1–8
19. Wilke N, Simm C, Zhang J, Ellermann J, Ya X, Merkle H, Path G, Ludemann H, Bache RJ, Ugurbil K (1993) Contrast-enhanced first pass myocardial perfusion imaging: correlation between myocardial blood flow in dogs at rest and during hyperemia. *Magn Reson Med* 29:485–497